A SPARSE APPROACH TO ASTRONOMICAL POINT SOURCE DETECTION

D. Herranz[1], *F. Argüeso*[2], *J. L. Sanz*[1] *and M. López-Caniego*[1]

[1] Instituto de Física de Cantabria, CSIC-UC, Av. los Castros s/n, 39005, Santander, Spain
[2] Departamento de Matemáticas, Universidad de Oviedo, 33007, Oviedo, Spain

ABSTRACT

In this work we introduce a method for the detection of point sources in images based on a l_1-norm sparse approximation. The method is inspired on astronomical image analysis but is directly applicable to any kind of images. We introduce a 'top-to-bottom' detection algorithm that can greatly reduce the computational burden of detection if the images are sufficiently well-behaved, in the sense that sources are truly sparse and the chances of source overlapping are small. We test our ideas with simulated faint sources embedded in white noise, comparing the results with the matched filter detector for a number of detection thresholds. We show that the sparse detection approach leads to better results in the ROC curve than the matched filter detector. Moreover, with the sparse approach it is possible to provide an objective stopping criterion for the detection algorithm.

1. INTRODUCTION

Over the last few years, theoretical advances in sparse representations have highlighted their potential to impact all fundamental areas of signal processing, from blind source separation to feature extraction and classification, denoising, and detection. In this context, finding a representation of a signal as a linear combination of a small number of elements from an over-complete set of vectors (dictionary) can clearly facilitate the detection, identification and separation problems.

An immediate application of these ideas lies in the field of astronomy. Let us consider a digital image of deep space: most of the pixels of the image are blank, whereas a small fraction of it contain the interesting features of the image: stars, faint nebulae and galaxies, globular clusters... In the optical region of the electromagnetic spectrum, a typical astronomical image is the perfect example of a sparse matrix. The same applies to most of the other bands relevant to astronomy, with significant exceptions such as the microwave and sub-mm bands where pervasive astronomical backgrounds appear in all pixels of the image. Even in those cases, it is still possible to find sparse representations of some of the interesting astrophysical signals (for example, point sources). Taking the previous considerations into account, it is not surprising that in the last few years sparse methodologies have started to be applied in many fields of astronomy, including the detection of periodical signals from sparse/incomplete sampled observations [22], source detection in low-count Poisson noise [21], applications of compressed sensing to the design of interferometric telescopes [6, 26], image inpainting [1], point spread function reconstruction [20], de-blurring [16] and many other applications.

In this work we are interested in the detection of point sources –i.e. signals that have a compact support in a small region of the the space (or time) domain– in additive noise. Two examples of interest in astronomy are the detection of faint stars in deep sky images and the detection of extragalactic objects in Cosmic Microwave Background (CMB) images. Specially in the later case, the point sources are embedded in a noisy background that makes them very hard to detect. Extragalactic point sources are the principal source of contamination for the CMB at small angular scales [7]. On the other hand, the physical and statistical properties of extragalactic sources at microwave frequencies are poorly known [8]. Therefore, in the last years a big effort has been devoted to the development of signal processing techniques specifically tailored for the detection of these objects in microwave astronomy [14].

A sparse approximation to the detection of point sources in one-dimensional data streams was recently introduced by [19]. In this work we extend these ideas to noisy two-dimensional images, focusing in the widespread white noise case. The structure of the paper is as follows: in section 2 we will review the proposed sparse methodology, based on the l_1 norm. We will also propose an algorithm that indicates how to proceed in front of any particular image where the presence of point souces is suspected. In section 3 we will study the performance of the proposed algorithm with simulations, comparing it with the standard matched filter detector. Finally, in section 4 we will draw our conclusions.

2. THE SPARSE METHODOLOGY

2.1 Data model

As usual, let us consider a set of data $\mathbf{d}(\vec{x})$, where $\vec{x}$ indicates the coordinates of an observation in the sky. Typically, the data samples $\mathbf{d}$ are arranged in a two-dimensional image, each pixel defined by a pair of coordinates (x^1, x^2). For convenience, it will be useful to rearrange the two dimensional data matrix into a single column vector of lexicographically ordered data, so that $\mathbf{d}$ is described by an $N \times 1$ matrix, with N the number of pixels of the image. The data contain a signal $\mathbf{s}$ linearly corrupted by a noise $\mathbf{z}$:

$$\mathbf{d} = \mathbf{s} + \mathbf{z}. \tag{1}$$

In the previous equation, $\mathbf{d}$, $\mathbf{s}$ and $\mathbf{z}$ are $N \times 1$ matrices of lexicographycally indexed elements. We shall assume that the noise has zero mean and has correlation matrix $\xi = [\xi_{ij}]$

$$\xi = \langle \mathbf{z}\mathbf{z}^t \rangle. \tag{2}$$

If the noise is statistically homogeneous and isotropic, the element ξ_{ij} of the correlation matrix depends only on the distance between pixels i and j. If the noise is white, ξ is a diagonal matrix. None of these two assumptions are necessary for this discussion, but if they are verified the calculations

 ISSN 2076-1465

are much simpler. Another assumption about the noise that is not necessary, but can simplify calculus, is Gaussianity.

Regarding the signal, for the purposes of this work it is the sum of a unknown number n of point sources:

$$\mathbf{s}(\vec{x}) = \mathbf{s}(x^1, x^2) = \sum_{\alpha=1}^{n} A_\alpha \delta(x^1 - x^1_\alpha, x^2 - x^2_\alpha), \qquad (3)$$

where A_α is the (positive) amplitude of the point source α and (x^1_α, x^2_α) are its *a priori* unknown coordinates. The point sources are observed by a telescope characterized by a point spread function (psf) ϕ, therefore the actual observed signal is

$$\mathbf{s}(\vec{x}) = \mathbf{s}(x^1, x^2) = \sum_{\alpha=1}^{n} A_\alpha \phi(x^1 - x^1_\alpha, x^2 - x^2_\alpha). \qquad (4)$$

In most CMB experiments, the psf ϕ is well described by a Gaussian beam profile. We can change the coordinates in both equations (3) and (4) to the same lexicographic indexes and write in a more compact form:

$$\mathbf{s} = \sum_{\alpha=1}^{n} A_\alpha \phi_\alpha. \qquad (5)$$

Let Φ be the $N \times n$ matrix whose columns are the lexicographically ordered versions of n replicas of ϕ, each shifted to the source locations (x^1_α, x^2_α) and $\mathbf{A}$ the $n \times 1$ vector whose elements are the amplitudes A_α. Then equation (1) becomes

$$\mathbf{d} = \Phi \mathbf{A} + \mathbf{z}. \qquad (6)$$

2.2 Sparse least l_p-norm approach

The matrix Φ in (6) is a *dictionary* formed by the n column vectors ϕ_α. In a typical astronomical image, the number of resolved sources that can be detected is much smaller than the number of pixels of the image, $n << N$. This leads naturally to the notion of *sparsity*. Thus the problem of detecting point sources embedded in additive noise can be formulated as the search for a sparse solution to equation (6) with a positivity constrain ($A_\alpha > 0$ for $\alpha = 1, \ldots, n$).

In recent years, sparse problems have been in the spotlight in mathematical literature [5, 9, 10, 11, 3, 4, 23, 25]. The most frequently used approach to sparse problems consists on the minimization of the norm l_p assuming a constraint on the goodness-of-fit. The l_p-norm of a vector $\mathbf{v}$ is

$$||\mathbf{v}||_p \equiv \left[\sum_\alpha |v_\alpha|^p \right]^{1/p}. \qquad (7)$$

Typical values of p include 0,1,2..., but even non-integer values can be used. Strictly speaking, the value of p that is directly connected to the notion of sparsity is $p = 0$ (minimizing the l_0-norm is equivalent to minimizing the number n of elements in the dictionary). However, in most cases $p = 0$ leads to a non-convex problem that is very difficult to solve. A possible solution is to consider the case $p \to 0$, as it was done in [19]. Fortunately, in many cases it can be shown that the case $p = 1$ leads to a solution that is very close to sparsity, with a much lower mathematical and computational cost.

Regarding the goodness-of-fit part of the problem, it takes the usual form

$$\varepsilon = (\mathbf{d} - \mathbf{s})^t \, \xi^{-1} \, (\mathbf{d} - \mathbf{s}). \qquad (8)$$

Thus, the l_p-norm takes the compact form

$$L_{p,\delta}: \ \min_{A>0} ||\mathbf{A}||_p \ \text{ s.t. } \ \varepsilon \leq \delta N, \qquad (9)$$

where δ is a regularization parameter. As discussed in [19], appropiate values for the regularization parameter are $\delta \sim 1$, and for the purposes of our work we can safely take $\delta = 1$. However, for the sake of completeness in the following discussion we will keep δ in all the equations.

Following the work by [19], the problem (9) is equivalent to the minimization of the constrained Lagrangian

$$\mathscr{L}(\mathbf{A}) = \frac{1}{2} \left(\mathbf{A}^t \mathbf{M} \mathbf{A} - 2 \mathbf{D}^t \mathbf{A} \right) + \lambda ||\mathbf{A}||_p^p, \qquad (10)$$

subject to the goodness-of-fit constraint

$$\varepsilon = \mathbf{A}^t \mathbf{M} \mathbf{A} - 2 \mathbf{D}^t \mathbf{A} + f \leq \delta N. \qquad (11)$$

In the previous equations,

$$\mathbf{M} \equiv \Phi^t \xi^{-1} \Phi, \qquad (12)$$

$$\mathbf{D} \equiv \Phi^t \xi^{-1} \mathbf{d}, \qquad (13)$$

$$f \equiv \mathbf{d}^t \xi^{-1} \mathbf{d}. \qquad (14)$$

Therefore, $\mathbf{M}$ is a $n \times n$ matrix, D is a $n \times 1$ vector and f is an scalar. Finally, in (10) λ is a Lagrangian multiplier that must satisfy a positivity constraint, $\lambda > 0$. The solution of (10) under the constraint (11) leads to the equations:

$$\sum_\beta M_{\alpha\beta} A_\beta + \lambda p A_\alpha^{p-1} = D_\alpha, \qquad (15)$$

$$\lambda = \left[p \sum_\alpha A_\alpha^p \right]^{-1} \times \left[f - \mathbf{D}^t \mathbf{A} - \delta N \right]. \qquad (16)$$

2.3 Solution for the l_1-norm

The case $p = 1$ is a convex problem that leads to analytical solutions. Let $\mathbf{e}$ be a vector of ones in $\mathbb{R}^n$, $\mathbf{e}^t = (1, \ldots, 1)$. Then the solutions of (15) and (16) for the case $p = 1$ are

$$\mathbf{A} = \mathbf{M}^{-1} (\mathbf{D} - \lambda \mathbf{e}), \qquad (17)$$

$$\lambda = \left[\frac{\mathbf{D}^t \mathbf{M}^{-1} \mathbf{D} + \delta N - f}{\mathbf{e}^t \mathbf{M}^{-1} \mathbf{e}} \right]^{1/2}. \qquad (18)$$

2.4 A sparse l_1-norm algorithm for the detection of point sources

We would like to remark that solutions (17-18) have little utility if the number n of sources is not known. Fortunately, the constraints on the positiveness of $\mathbf{A}$ and λ can help us to solve the problem.

A naïve algorithm would start by considering all the N pixels in the image, solving equations (17) and (18) and checking if all the elements of $\mathbf{A}$ and λ are positive. If, as is expected, the conditions are not satisfied, then the algorithm would repeat the same procedure with $N - 1$ points, check again, then do it again with $N - 2$ pixels, and continue so on until the constraints on $\mathbf{A}$ and λ are satisfied.

There are two problems with this naïve approach. The first one is computational cost. Even for a moderate sized

image, let us say a 256×256 pixels one, the size of matrices ξ and $\mathbf{M}$ would be huge (in the considered example, 65536×65536 elements). Even considering all the possible symmetries and simplifications of the problem (for example white, homogeneous and isotropic noise, etc) the total number of operations would be prohibitive.

The second problem is more subtle, and it is related to the decision of how to get out pixels from the sample in each iteration. A seemingly natural option would be to start from the lowest value pixel and proceed in ascending order, but nothing tells us this is the most efficient path. Even if this procedure would lead us to a solution (provided enough CPU power and time), it is not proven that such a solution is the one with a minimum number n of sources among the possible solutions. Once the positivity conditions are met it could be still possible to find solutions with smaller number of sources, or other configurations with the same number of sources but better goodness-of-fit. In other words, going 'upwards' from a large to a smaller n does not necessarily guarantee the sparsest solution.

A possible solution to overcome this problem is the use of smart sampling algorithms specifically designed for the case of unknown number of sources, such as the Reversible Jump Markov Chain Monte Carlo method [13]. In this work, however, we propose a simpler algorithm inspired on the detection procedure that is most commonly used in astronomy.

In typical astronomical images most point sources, or at least the brighter ones, are found in 'hot pixels' of the image or nearby. This is particularly true after the image is convolved with a linear filter such as the matched filter or a wavelet [see for example 24, 2, 18, 12]. A common practice in astronomy is to filter the data in order to enhance the point sources and then to identify regions above a certain threshold (usually the celebrated 5σ level) as detections. Keeping a sufficiently high threshold guarantees a high significance of the detection. This methodology is well established and has proven to be very succesful in CMB astronomy [17, 15]. The main objection to thresholding is that the choice of the threshold is arbitrary. However, we know that the brighter peaks of the filtered image are an excellent guess of the locations of point sources. Since the l_p-norm minimization leads to the quantity $\mathbf{D}$ that is proportional to the matched filtered image, our algorithm starts with the matched filter:

1. If the noise correlation matrix ξ is not known, estimate it from the data. Calculate f.
2. Filter the image with the matched filter (13).
3. Locate the local maxima of the filtered image and sort them downwards from larger to smaller values.
4. Set $n = 1$.
5. Take the positions and intensities of the first n peaks from the ordered list of maxima and construct the corresponding vector $\mathbf{D}$ and the matrix $\mathbf{M}$.
6. Obtain estimates for $\mathbf{A}$ and λ using equations (17) and (18).
7. Check the positivity constraint of $\mathbf{A}$ and λ. If the constraint is not satisfied, make $n = n + 1$ and go back to step 5. If the constraint is satisfied, exit the algorithm.

If point sources are truly sparse (few in comparison with the number of pixels of the image), bright enough (so that the can be identified by peaks in the filtered image) and do not overlap among themselves, the previous algorithm converges to a solution of (9) in the sense that it finds the minimum number of elements of the dictionary, located at the positions of the local maxima of the filtered image, that satisfy the constrains of positivity and goodness-of-fit. Going downwards from brighter to fainter pixels and increasing the number of candidates by one at each step guarantees sparsity. Moreover, the algorithm tells us when to stop going down, thus avoiding the arbitrarity of the thresholding method. Since the iterations usually stop before the number n of candidates becomes too large, the algorithm is fast and computationally inexpensive. The overall computational burden is equivalent to $\sim \mathcal{O}(n^2)$ times the operations needed for a single matched filter, where n is the number of sources detected by the method.

3. TESTING THE ALGORITHM

In this section we will test the proposed l_1-norm algorithm with simulations, comparing it with the standard matched filter thresholding method. We will focus, as figure of merit, on the receiver operating characteristic (ROC) curves for each method. The ROC curve shows the fraction of true positives (TPR) as a function of the fraction of false positives (FPR), where

$$\text{TPR} = \frac{\text{true positives}}{\text{true positives} + \text{false negatives}} \quad (19)$$

$$\text{FPR} = \frac{\text{false positives}}{\text{false positives} + \text{true negatives}}. \quad (20)$$

True positives are identified as peaks accepted by our detection criterion that lie within a circle of 1 FWHM radius centered in the position of any of the simulated sources. False positives are peaks accepted by our detection criterion that have no counterpart among the simulated sources. A false negative or 'miss' is a peak that has not satisfied our detection criterion but corresponds to one of the simulated sources, whereas a true negative is a peak that has not satisfied our detection criterion and is caused not by a simulated source, but by the noise fluctuations instead.

We simulate white, uniform Gaussian noise. In this case, the noise correlation matrix is diagonal, $\xi = \text{diag}(\sigma^2, \ldots, \sigma^2)$. For simplicity, we set $\sigma = 1$ (in arbitrary units) and then ξ is just the identity $N \times N$ matrix. In order to lighten as much as possible the computational burden of the test, we simulate small images: $N = 64 \times 64 = 1024$ pixels. Over each noise realization we place four identical point sources, arranged in a square with fixed corners in order to avoid any possibility of overlap between the sources. The point sources have Gaussian profile with a width of 2 pixels (FWHM=4.71 pixels) and identical amplitudes $\mathbf{A}_0 = 1$ (in the same arbitrary units of the noise map), therefore the sources have a SNR=$A_0/\sigma = 1$. We perform 1000 of these simulations, changing the noise realization each time.

For each simulation we apply a matched filter and we look for peaks above a certain threshold, thus obtaining the number of detections for that threshold. The intensity of the peak (after the appropiate renormalization) is taken as the estimation of the source amplitude. We also check how many of these detections are true and how many are spurious. In order to decide whether a candidate is a true or spurious detection, we apply a proximity criterion: if the candidate lies in a circle whose radius is $r = \text{FWHM}/2$, centered at the true position of one of the four sources we introduced in the image,

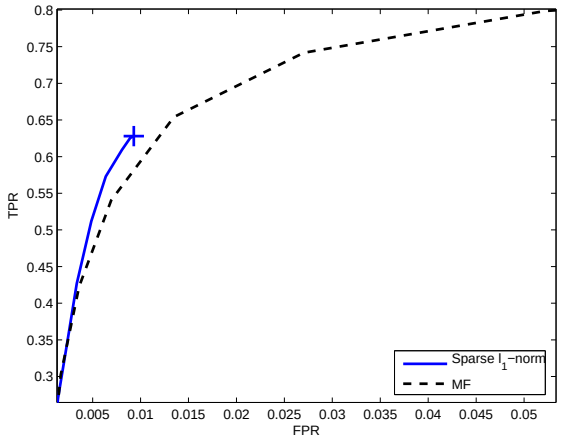

Figure 1: ROC curves for 1000 simulated images. The dashed line shows the TPR as a function of FPR for the matched filter. The solid line shows the same curve for our proposed algorithm. The solid cross indicates the final result for our proposed algorithm.

we consider the candidate as a valid detection. Otherwise, it is considered a spurious detection. Since the results are dependent of the threshold, we calculate the number of true and spurious detections for a number of different threshold values, ranging from $t = 0$ to $t = 2$ (always in our arbitrary units). This way we can construct the ROC curve for the selected detection method. In order to have enough statistics, we construct the curve not for a single realization, but for the sum of the 1000 simulations.

We repeat the same for our l_1-norm top-to-bottom detection algorithm. The difference is that the algorithm fixes by itself the threshold where it must stop. Therefore, it gives a single number of true (true positive) and spurious (false positive) detections, instead of a curve depending on the threshold as in the case of the matched filter. In order to facilitate the graphical comparison with the matched filter, we can obtain the rest of points of the ROC curve by artificially stopping the algorithm at higher intensity thresholds. For this plot we use the same intensity thresholds we tested with the matched filter. Please note once more that these thresholds are artificial in our l_1-norm scheme and have been used only for illustrative purposes.

Figure 1 shows the ROC curves for 1000 simulations with Gaussian white noise. The dashed line indicates the results obtained with the matched filter plus thresholding. Each point of the curve corresponds to a different threshold (higher thresholds to the left of the diagram). The dashed curve continues to grow to the right of the diagram, but the plot has been cut for the sake of clarity. The solid line indicates the results obtained with our sparse l_1-norm method. Strictly speaking, the algorithm gives only one point of the diagram: this is indicated by a solid cross (+) at the end of the solid curve. In order to better compare with the matched filter, higher thresholds are selected artificially in order to complete the curve.

Figure 1 must be interpreted in the following way: the dashed curve runs below the continuos line. This means that for any fixed number of true detections, our sparse method leads to a lower number of false detections. In other words, the sparse method is not only able to determine by itself when to stop, but also controls the number of false positives better than simple thresholding.

4. CONCLUSIONS

In this work we have introduced a method for the detection of point sources in images based on a l_1-norm sparse approximation. The detection of pointlike objects is a common problem in Astronomy, being a typical example the detection of stars, far galaxies and/or galaxy clusters in deep space observations. Although in this paper we have used as an example the case of astronomic image processing, the method we introduce can be applied to any kind of images where pointlike signals are present.

In a typical astronomical image, the number of resolved sources that can be detected is much smaller than the number of pixels. This leads naturally to the notion of sparsity. In a sparse model, the relevant signal can be described in terms of a small number of elements of a dictionary. In our case, the dictionary is formed by shifted replicas of the point source characteristic point spread function, that is, its spatial template, that we assume that is constant across the image.

For this work, we have considered a minimization of the l_1-norm assuming a constraint on the goodness-of-fit plus a positivity constraint on the intensity of the sources. We have chosen the l_1 norm because the associated sparse problem is convex. Moreover, the l_1-norm problem allows us to obtain analytical formulas. We have obtained the expressions that solve the problem and we have proposed a very simple and intuitive algorithm that proceeds downwards from the brightest to the faintest image peaks for the detection of point sources in Gaussian noise. An important feature of the algorithm is that it provides an objective criterion in order to decide where to stop the search for new sources.

We have tested our algorithm in 1000 simulations with Gaussian white noise, introducing toy point sources and comparing the performance of our proposed algorithm with the performance of the standard matched filter detector. We have obtained the numbers of detections and false positives for the two methods and constructed the corresponding ROC curves. Strictly speaking, our downwards sparse detection algorithm gives only one point of the diagram; in order to complete the ROC curve, higher detection thresholds have been selected artificially. Our results show that the proposed algorithm leads to a better ratio between true and false positives for the case of white Gaussian noise. The more general case of color noise will be addressed in a future work.

Acknowledgments

The authors acknowledge partial financial support from the Spanish Ministry of Education (MEC) under project ESP2004-07067-C03-01 and from the joint CNR-CSIC research project 2008IT0059. MLC acknowledges an EGEE-III postdoctoral contract at IFCA.

References

[1] P. Abrial, Y. Moudden, J. Starck, J. Fadili, J. Delabrouille, and M. K. Nguyen. CMB data analysis and sparsity. *Statistical Methodology*, 5:289–298, July 2008.

[2] R. B. Barreiro, J. L. Sanz, D. Herranz, and E. Martínez-González. Comparing filters for the detection of point sources. *MNRAS*, 342:119–133, June 2003.

[3] J. Bobin, Y. Moudden, J. Starck, and M. Elad. Morphological diversity and source separation. *IEEE Signal Processing Letters*, 13(7):409–412, July 2006.

[4] J. Bobin, J.-L. Starck, Y. Moudden, and M. J. Fadili. Blind Source Separation: The Sparsity Revolution. In *Advances in Imaging and Electron Physics*, volume 152 of *Advances in Imaging and Electron Physics Series*, pages 221–302. 2008.

[5] E. Candés, J. Romberg, and T. Tao. Stable signal recovery from incomplete and inaccurate measurements. *Commun. Pure Appl. Math.*, 59(8):1207–1223, Aug. 2006.

[6] K. G. Carpenter, K. Gendreau, J. Leitner, R. Lyon, E. Stoneking, H. P. Stahl, J. Parrish, C. J. Schrijver, R. Woodruff, C. Lillie, A. Lo, D. Mozurkewich, A. Labeyrie, D. Miller, K. Mighell, M. Karovska, J. Phillips, R. J. Allen, and W. Cash. Technology Development for Future Sparse Aperture Telescopes and Interferometers in Space. In *AGB Stars and Related Phenomenastro2010: The Astronomy and Astrophysics Decadal Survey*, volume 2010 of *Astronomy*, pages 47–+, 2009.

[7] G. de Zotti, R. Ricci, D. Mesa, L. Silva, P. Mazzotta, L. Toffolatti, and J. González-Nuevo. Predictions for high-frequency radio surveys of extragalactic sources. *A&A*, 431:893–903, Mar. 2005.

[8] G. de Zotti, L. Toffolatti, F. Argüeso, R. D. Davies, P. Mazzotta, R. B. Partridge, G. F. Smoot, and N. Vittorio. The Planck Surveyor Mission: Astrophysical Prospects. In L. Maiani, F. Melchiorri, and N. Vittorio, editors, *3K cosmology*, volume 476 of *American Institute of Physics Conference Series*, pages 204–+, 1999.

[9] D. Donoho, M. Elad, and V. Temlyakov. Stable recovery of sparse overcomplete representations in the presence of noise. *IEEE Transactions on Information Theory*, 52(1):6–18, Jan. 2006.

[10] A. K. Fletcher, S. Rangan, V. K. Goyal, and K. Ramchandran. Denoising by sparse approximation: Error bounds based on rate-distortion theory. *EURASIP J. Appl. Signal Process.*, pages 1–19, 2006.

[11] J.-J. Fuchs. Recovery conditions of sparse representations in the presence of noise. In *2006 IEEE International Conference on Acoustics, Speech, and Signal Processing, Vol III, Proceedings*, International Conference on Acoustics Speech and Signal Processing (ICASSP), pages 337+, 2006. 31st IEEE International Conference on Acoustics, Speech and Signal Processing, Toulouse, France, May 14-19, 2006.

[12] J. González-Nuevo, F. Argüeso, M. López-Caniego, L. Toffolatti, J. L. Sanz, P. Vielva, and D. Herranz. The Mexican hat wavelet family: application to point-source detection in cosmic microwave background maps. *MNRAS*, 369:1603–1610, July 2006.

[13] P. J. Green. Reversible jump markov chain monte carlo computation and bayesian model determination. *Biometrika*, 82(4):711–732, Dec. 1995.

[14] D. Herranz and P. Vielva. Cosmic microwave background images. *Signal Processing Magazine, IEEE*, 27(1):67–75, Jan. 2010.

[15] G. Hinshaw, M. R. Nolta, C. L. Bennett, R. Bean, O. Doré, M. R. Greason, M. Halpern, R. S. Hill, N. Jarosik, and A. Kogut. Three-Year Wilkinson Microwave Anisotropy Probe (WMAP) Observations: Temperature Analysis. *ApJS*, 170:288–334, June 2007.

[16] B. D. Jeffs and M. Gunsay. Restoration of blurred star field images by maximally sparse optimization. *IEEE Transactions on Image Processing*, 2:202–211, Apr. 1993.

[17] M. López-Caniego, J. González-Nuevo, D. Herranz, M. Massardi, J. L. Sanz, G. De Zotti, L. Toffolatti, and F. Argüeso. Nonblind Catalog of Extragalactic Point Sources from the Wilkinson Microwave Anisotropy Probe (WMAP) First 3 Year Survey Data. *ApJS*, 170:108–125, May 2007.

[18] M. López-Caniego, D. Herranz, R. B. Barreiro, and J. L. Sanz. A Bayesian approach to filter design: detection of compact sources. In C. A. Bouman and E. L. Miller, editors, *Computational Imaging II. Edited by Bouman, Charles A.; Miller, Eric L. Proceedings of the SPIE, Volume 5299, pp. 145-154 (2004).*, volume 5299 of *Presented at the Society of Photo-Optical Instrumentation Engineers (SPIE) Conference*, pages 145–154, May 2004.

[19] F. Martinelli and J. Sanz. Sparse representations versus the matched filter. In Rémi Gribonval, editor, *SPARS'09 - Signal Processing with Adaptive Sparse Structured Representations*, Saint Malo, France, 2009. Inria Rennes - Bretagne Atlantique.

[20] F. Rooms, W. R. Philips, and J. Portilla. Parametric PSF estimation via sparseness maximization in the wavelet domain. In F. Truchetet & O. Laligant, editor, *Society of Photo-Optical Instrumentation Engineers (SPIE) Conference Series*, volume 5607 of *Presented at the Society of Photo-Optical Instrumentation Engineers (SPIE) Conference*, pages 26–33, Nov. 2004.

[21] J. Starck, J. M. Fadili, S. Digel, B. Zhang, and J. Chiang. Source detection using a 3D sparse representation: application to the Fermi gamma-ray space telescope. *A&A*, 504:641–652, Sept. 2009.

[22] E. Tilton, C. L. Mancone, and A. Sarajedini. Variable Star Period Determination for Datasets with Sparse Time Sampling. In *American Astronomical Society Meeting Abstracts*, volume 215 of *American Astronomical Society Meeting Abstracts*, pages 418.08–+, Jan. 2010.

[23] J. A. Tropp. Just relax: Convex programming methods for identifying sparse signals in noise (vol 51, pg 1030, 2006). *IEEE Trans. Inf. Theory*, 55(2):917–918, Feb. 2009.

[24] P. Vielva, E. Martínez-González, J. E. Gallegos, L. Toffolatti, and J. L. Sanz. Point source detection using the Spherical Mexican Hat Wavelet on simulated all-sky Planck maps. *MNRAS*, 344:89–104, Sept. 2003.

[25] M. J. Wainwright. Sharp thresholds for high-dimensional and noisy sparsity recovery using l_1-constrained quadratic programming (lasso). *IEEE Trans. Inf. Theory*, 55(5):2183–2202, May 2009.

[26] Y. Wiaux, L. Jacques, G. Puy, A. M. M. Scaife, and P. Vandergheynst. Compressed sensing imaging techniques for radio interferometry. *MNRAS*, 395:1733–1742, May 2009.